Journal of Solid State Chemistry **163,** 210–217 (2002)
doi:10.1006/jssc.2001.9394, available online at http://www.idealibrary.com on IDEAL®

A New Vanadium–Molybdenum Mixed Bronze Family with a Tunnel Structure: The Phases $A_x(Mo,V)_8O_{21}$ ($A = K^+$, Rb^+, Cs^+)

P. Millet,[1] C. Gasquères, and J. Galy

Centre d'Elaboration de Matériaux et d'Etudes Structurales, CEMES-CNRS, 29 rue Jeanne Marvig, BP 4347, 31055 Toulouse Cedex 4, France

Received June 27, 2001; in revised form August 29, 2001; accepted September 7, 2001

The isostructural compounds of general formula $A_x(Mo, V)_8O_{21}$ ($A = K^+$, Rb^+, Cs^+) have been synthesized by solid state reaction. They crystallize in the monoclinic system, space group $I2/m$, $Z = 2$, within the case of K^+: $a = 16.194(2)$ Å, $b = 13.716(1)$ Å, $c = 13.716(1)$ Å, and $\beta = 90.983(1)^\circ$. The three-dimensional network is built up by layers parallel to the (101) plane, constituted of two triple chains of MO_6 octahedra (M = Mo, V) associated by edges along the [010] direction and sharing corners in the $[\bar{1}0\bar{1}]$ direction, which are connected in the [001] direction via double chains of edge-sharing VO_5 square pyramids. This leads to large tunnels where the alkali ions are located. This family provides a new example of a mixed vanadium–molybdenum bronze. © 2002 Elsevier Science

Key Words: **molybdenum–vanadium bronzes; X-ray diffraction; crystal structure; tunnel structure.**

INTRODUCTION

In the search for new materials presenting improved ionic or magnetic properties, the possibility to synthesize new compounds with tunnel structures was investigated. This work was motivated by the recent discovery of the fascinating $Na_2V_3O_7$ crystal structure where isolated vanadium (IV)–oxygen nanotubes are present (1). It is worth noting that this unique compound is not the only one, among the vanadates, to be formed of isolated tunnels built up of edge- and corner-shared VO_5 square pyramids (SP). $Cs_{0.3}V_2O_5$ (2) can also be seen in such a way if as the long vanadium–oxygen distances are not considered. However, the main difference between the two structures is that VO_5 SP apices all point out from the nanotubes in $Na_2V_3O_7$ whereas they point alternatively in and out in $Cs_{0.3}V_2O_5$.

The concept—first put forward in the case of zeolite frameworks (3, 4) and then extended to understand the existence of various $M_xV_2O_5$ solid solution phases (5)—that particular frameworks, typically either tunnel structures or two-dimensional layer structures, possess inherent structural flexibility was applied here as a new synthesis approach. The assumption was that tunnel structures, such as the ones existing in $A_xV_2O_5$, could be obtained if ions of large ionic radius were put in the presence of a layer compound already having the desired geometry; the cation (A), following the oxygen bonding distances criterion, would, a priori, determine how the framework will accommodate it.

In the case of $Cs_{0.3}V_2O_5$, it was found that the layer compound $(Mo_{0.3}V_{0.7})_2O_5$ (6) was actually meeting the above-mentioned requirements. Its layer structure derives from V_2O_5 by simple rotation of one over two VO_5 SP double chains.

Here we report the results of our first investigation when mixtures of $M_2C_2O_4$ ($M = K^+, Rb^+, Cs^+$) and $(Mo_{0.3}V_{0.7})_2O_5$ are used as starting materials. Synthesis conditions and single-crystal structure determinations of a new tunnel structure family of general formula $A_x(V,Mo)_8O_{21}$ are presented.

EXPERIMENTAL

The $(Mo_{0.3}V_{0.7})_2O_5$ precursor was prepared by solid state reaction as follows. A stoichiometric mixture of MoO_3, V_2O_5, and V_2O_3 (prepared by reducing V_2O_5 under hydrogen at 800°C) was ground in an agate mortar and then annealed in a vacuum-sealed quartz tube at 575°C for 12 h.

Powder samples of $A_x(Mo,V)_8O_{21}$ were obtained by solid state reaction starting from a mixture of alkali oxalates $A_2C_2O_4$ ($A = K^+$, Rb^+, Cs^+) and $(Mo_{0.3}V_{0.7})_2O_5$ in the molar ratio 1:6. All thermal treatments were performed in two steps: the first one, at 250°C for 1 h under dynamic vacuum, to remove the carbon dioxide coming from the oxalate decomposition and the second one, under static vacuum at various temperatures. The different experiments are listed in Table 1. The samples were analyzed by X-ray powder diffraction. The results show that experimental conditions have to be adjusted depending on the alkali element used. In the case of K^+ and Rb^+, single phases can be obtained at temperature around 650°C and relatively short

[1] To whom correspondence should be addressed. Fax: 33 5 62 25 79 99. E-mail: millet@cemes.fr.

0022-4596/02 $35.00
© 2002 Elsevier Science
All rights reserved.

TABLE 1
Different Experiments Performed and Indexation of X-Ray Diffractograms

A	Reference	Dwell time (h)	Temperature (°C)	XRD analysis
K^+	KM01	12	500	$K_2Mo_3O_{10}$[a] + unknown
	KM02	1	550	$A_x(Mo,V)_8O_{21}$ + unknown
	KM03	1	600	$A_x(Mo,V)_8O_{21}$ + unknown
	KM04	1	650	$A_x(Mo,V)_8O_{21}$
	Optimum crystallization	3	600	
Rb^+	RbM01	12	500	$A_x(Mo,V)_8O_{21}$ + unknown
	RbM02	1	600	$A_x(Mo,V)_8O_{21}$ + unknown
	RbM03	1	650	$A_x(Mo,V)_8O_{21}$
	RbM04	6	650	$A_x(Mo,V)_8O_{21}$
	RbM05	12	650	$A_x(Mo,V)_8O_{21}$
	Optimum crystallization	9	650	
Cs^+	CsM01	12	500	$A_x(Mo,V)_8O_{21}$
	CsM02	3	585	$A_x(Mo,V)_8O_{21}$
	CsM03	6	585	$A_x(Mo,V)_8O_{21}$
	CsM04	9	585	$A_x(Mo,V)_8O_{21}$ + $Cs_{0.13}V_{0.13}Mo_{0.87}O_3$[b]
	CsM05	1	600	$A_x(Mo,V)_8O_{21}$ + $Cs_{0.3}V_2O_5$[c] + $Cs_{0.35}V_3O_7$[d]
	CsM06	12	600	$A_x(Mo,V)_8O_{21}$ + $Cs_{0.13}V_{0.13}Mo_{0.87}O_3$[b]
	Optimum crystallization	9	585	

JCPDS file number: [a]37-1467; [b]27-1092; [c]70-0325; [d]70-0324.

annealing times. For Cs^+, results depend on both annealing temperature and annealing time. The optimum temperature is close to 585°C but if the annealing time is too long, i.e., 6 h, a multiphase mixture which consists of $A_x(Mo,V)_8O_{21}$ and the hexagonal phase $Cs_{0.13}V_{0.13}Mo_{0.87}O_3$ is obtained. At 600°C, short annealing time leads to a mixture where the

TABLE 2
Crystallographic Data for the $A_{2-x}V^{5+}_{8-x-2y}V^{4+}_yMo^{6+}_{x+y}O_{21}$ Phases with A = K, Rb, Cs

	A		
Crystal data	K	Rb	Cs
System	Monoclinic	Monoclinic	Monoclinic
Space group	*I*2/*m*	*I*2/*m*	*I*2/*m*
a (Å)	16.194(2)	16.363(2)	16.497(3)
b (Å)	3.6340(2)	3.6340(2)	3.6300(3)
c (Å)	13.716(1)	13.726(1)	13.702(2)
β (°)	90.981(3)	91.242(3)	90.966(4)
V (Å^3)	807.1(1)	807.0(1)	820.5(2)
Z	2	2	2
Formula weight	856.46	896.61	918.19
ρ_{calc} (g/cm^3)	3.524	3.649	3.717
$\mu_{MoK\alpha}$(cm^{-1})	96.6	153.3	134.6
Dimension (mm)	$0.026 \times 0.0212 \times 0.1325$	$0.053 \times 0.053 \times 0.153$	$0.0159 \times 0.0145 \times 0.106$
Color	Dark brown	Dark brown	Dark brown
Experimental details			
Temperature (°C)	293.2	293.2	293.2
Wavelength (Mo$K\alpha$)	0.71069	0.71069	0.71069
Max. Bragg angle (°)	32°	32°	32°
Collected reflections	2522	2623	1794
Data/restraints/parameters	1183/3/103	1149/3/103	797/3/103
$R = \sum\|\|F_o\| - \|F_c\|\|/\sum F_o$%	4.16	4.45	4.94
$R_w = [\sum w(\|F_o^2 - F_c^2\|)^2/\sum w(F_o^2)^2]^{1/2}$(%)	8.58	8.16	8.56
Goodness of fit on F^2	1.074	1.061	1.131
Weighting scheme/2 terms Chebychev	0.0419/0	0.0336/0	0/0
Large difference peak and hole (e.Å^3)	1.52/ − 1.69	1.23/ − 1.308	1.08/ − 1.08

TABLE 3
Atomic Coordinates, Thermal Parameters, and Site Occupancies in $A_{2-x}V^{5+}_{8-x-2y}V^{4+}_{y}Mo^{6+}_{x+y}O_{21}$ with A = K, Rb, Cs

Atoms		K	Rb	Cs	Atoms		K	Rb	Cs
A	x	0.0055(2)	0.0058(1)	0.0057(1)	O4	x	0.1798(2)	0.1790(3)	0.1789(4)
	y	0	0	0		y	$\frac{1}{2}$	$\frac{1}{2}$	$\frac{1}{2}$
	z	0.3607(2)	0.3693(2)	0.3693(2)		z	0.7240(3)	0.7232(3)	0.7225(4)
	$U_{eq.}$	0.065(2)	0.038(1)	0.0329(7)		$U_{eq.}$	0.017(1)	0.018(1)	0.017(1)
	τ_A	0.466(7)	0.429(3)	0.393(3)					
$M1$	x	0.39089(4)	0.39155(5)	0.39241(7)	O5	x	0.1055(2)	0.1095(5)	0.1126(4)
	y	$\frac{1}{2}$	$\frac{1}{2}$	$\frac{1}{2}$		y	$\frac{1}{2}$	$\frac{1}{2}$	$\frac{1}{2}$
	z	0.46777(4)	0.46817(5)	0.4683(1)		z	0.5453(3)	0.5416(3)	0.5418(5)
	$U_{eq.}$	0.0125(2)	0.0121(2)	0.0131(4)		$U_{eq.}$	0.025(1)	0.024(2)	0.025(2)
	τ_1	0.37(1)/ 0.63(1)	0.36(1)/ 0.64(1)	0.36(1)/ 0.64(1)					
$M2$	x	0.19922(4)	0.20161(5)	0.2035(1)	O6	x	0.2572(2)	0.2596(2)	0.2611(4)
	y	$\frac{1}{2}$	$\frac{1}{2}$	$\frac{1}{2}$		y	$\frac{1}{2}$	$\frac{1}{2}$	$\frac{1}{2}$
	z	0.58718(5)	0.58617(6)	0.5869(1)		z	0.4581(3)	0.4582(3)	0.4575(4)
	$U_{eq.}$	0.0133(3)	0.0124(3)	0.0123(5)		$U_{eq.}$	0.014(1)	0.011(1)	0.014(1)
	τ_2	0.23(1)/ 0.77(1)	0.21(1)/ 0.79(1)	0.17(1)/ 0.83(1)					
$M3$	x	0.13420(4)	0.13405(5)	0.1345(1)	O7	x	0.3886(2)	0.3892(3)	0.3908(4)
	y	$\frac{1}{2}$	$\frac{1}{2}$	$\frac{1}{2}$		y	$\frac{1}{2}$	$\frac{1}{2}$	$\frac{1}{2}$
	z	0.83735(5)	0.83599(5)	0.8362(1)		z	0.3487(3)	0.3493(3)	0.3493(5)
	$U_{eq.}$	0.0102(2)	0.0097(3)	0.0108(5)		$U_{eq.}$	0.018(1)	0.017(1)	0.019(1)
	τ_3	0.25(1)/ 0.75(1)	0.30(1)/ 0.70(1)	0.25(1)/ 0.75(1)					
V	x	0.22294(5)	0.22460(6)	0.2260(1)	O8	x	$\frac{1}{2}$	$\frac{1}{2}$	$\frac{1}{2}$
	y	$\frac{1}{2}$	$\frac{1}{2}$	$\frac{1}{2}$		y	$\frac{1}{2}$	$\frac{1}{2}$	$\frac{1}{2}$
	z	0.33291(6)	0.33279(7)	0.3336(1)		z	$\frac{1}{2}$	$\frac{1}{2}$	$\frac{1}{2}$
	$U_{eq.}$	0.0106(3)	0.0109(3)	0.0119(5)		$U_{eq.}$	0.016(2)	0.014(2)	0.014(2)
O1	x	0.3786(2)	0.3797(2)	0.3808(4)	O9	x	0.0368(2)	0.0371(3)	0.0391(4)
	y	0	0	0		y	$\frac{1}{2}$	$\frac{1}{2}$	$\frac{1}{2}$
	z	0.5050(3)	0.5046(3)	0.5062(4)		z	0.8111(3)	0.8092(3)	0.8094(5)
	$U_{eq.}$	0.012(1)	0.011(1)	0.013(1)		$U_{eq.}$	0.025(1)	0.023(1)	0.024(2)
O2	x	0.2262(2)	0.2290(3)	0.2293(4)	O10	x	0.1256(2)	0.1276(3)	0.1309(4)
	y	0	0	0		y	$\frac{1}{2}$	$\frac{1}{2}$	$\frac{1}{2}$
	z	0.5975(3)	0.5985(4)	0.5974(4)		z	0.3394(3)	0.3488(3)	0.3417(5)
	$U_{eq.}$	0.016(1)	0.015(1)	0.015(1)		$U_{eq.}$	0.022(1)	0.023(1)	0.024(2)
O3	x	0.1559(2)	0.1553(2)	0.1550(4)	O11	x	0.2492(2)	0.2503(3)	0.2506(4)
	y	0	0	0		y	0	0	0
	z	0.8750(3)	0.8738(3)	0.8741(5)		z	0.3073(2)	0.3083(3)	0.3075(5)
	$U_{eq.}$	0.015(1)	0.013(1)	0.014(1)		$U_{eq.}$	0.015(2)	0.015(1)	0.018(2)
Resulting values for x and y:									
	x	1.068	1.142	1.214					
	y	0.632	0.598	0.346					

A: potassium, rubidium, cesium. M: Mo and V sharing the same crystallographic site. τ: ratios Mo/V; total site occupancy = 1. For alkali cations $0 \leq \tau_A \leq 1$.

Crystal formulas: $K_{0.932}V^{5+}_{5.668}V^{4+}_{0.632}Mo^{6+}_{1.700}O_{21}$; $Rb_{0.858}V^{5+}_{5.662}V^{4+}_{0.598}Mo^{6+}_{1.740}O_{21}$; $Cs_{0.786}V^{5+}_{6.094}V^{4+}_{0.346}Mo^{6+}_{1.560}O_{21}$.

tunnel structure phases $Cs_{0.3}V_2O_5$ and $Cs_{0.35}V_3O_7$ are present, whereas longer annealing time leads again to the appearance of $Cs_{0.13}V_{0.13}Mo_{0.87}O_3$ in addition to $A_x(Mo,V)_8O_{21}$.

Single crystals were obtained by annealing $A_x(Mo,V)_8O_{21}$ powders at temperature close to that of the decomposition of the phases followed by a slow cooling (typically in the range from 3 to 5°C/h) to room temper-

ature. For the three compositions, needle-like crystals suitable for single-crystal X-ray diffraction study were isolated. Data were collected on an Enraf-Nonius four-circle diffractometer equipped with a KAPPA-CCD detector. The cell parameters were determined from the collection of 10 frames using the program Collect (7). SIR92 (8) was used to solve the structures by direct methods and refinements were performed using SHEXL-96 (9). An absorption correction was applied using the program SORTAV (10). The set of physical and crystallographic characteristics as well as the experiment conditions are listed in Table 2.

RESULTS

Structure Description

The three phases corresponding to $A = K^+$, Rb^+, and Cs^+ are isostructural. Atomic parameters and selected interatomic distances are listed in Tables 3 and 4, respectively. A projection of the structure onto the plane (010) is given in Fig. 1. All the atoms are located in the mirror planes of the space group $I2/m$ at $y = 0$ and $\frac{1}{2}$. Part of the basic unit of the three-dimensional network $[M_8O_{21}]_n$ is built up by three independent MO_6 octahedra, $M1O_6$ and $M2O_6$ sharing the edge O6–O3h and connected via O4 to $M3O_6$ octahedron; this entity is repeated by the symmetry center placed on oxygen O8 of the equatorial plane of the $M1O_6$ octahedron. All these six octahedra which form an S-shaped chain are in the mirror plane at $y = \frac{1}{2}$. Repeated by the twofold helicoidal axis 2_1, the same following unit along [010] is linked via the common edges O3h–O2 and O3h–O1 between $M3hO_6$ octahedra (at $y = 0$) with the double unit $M1O_6$ and $M2O_6$. This assembly develops along $[\bar{1}01]$ and [010] directions by corner and edge sharing, making a layer $[M_3O_{19}]_n$ parallel to the (101) plane. Grafted on the oxygens O6 and O6h of the double units $[M1O_6–M2O_6]$, the double strings $[V_2O_6]_n$ formed by the VO_5 square pyramids sharing O10–O11 edges along the 2_1 axis ensure the linkage between the $[M_3O_{19}]_n$ layers. Therefore, a large tunnel is formed, bordered by the O9, O4, O5, O10, O7k, O9i, O4i, O5i, O10i, and O7ki oxygen atoms admitting a twofold axis, in which A alkali atoms are distributed over two crystallographic sites, A and Ai, related by a symmetry center. A schematic drawing projected along the Oy axis is given in Fig. 2a. It shows the particular assembly of MO_6 and VO_5 polyhedra and illustrates this three-dimensional network.

The three MO_6 octahedra in which Mo and V are distributed with various ratios are rather distorted. All the M–O bonds pointing toward the tunnel, i.e., $M1$–O7, $M2$–O5, and $M3$–O9 being around 1.62 Å, possess a double bond character. Such a fact is classical in both molybdenum(VI) and vanadium(V) or -(IV) crystal chemistry. Opposite to these short bonds there are long ones, $M1$–O3h, $M2$–O3h, and $M3$–O2h around 2.35 Å, which result from the off-centering of M inside the oxygenated octahedra. Vanadium in the V site exhibits the same characteristics with the short V–O10 = 1.581 Å bond directed toward the tunnel. In the double string $[V_2O_6]_n$ the V–V = 3.044 Å distance through the common edge O11–O11k is shorter than all the M–M distances in the $[M_3O_{19}]_n$ layer by some 0.3 to 0.4 Å which indicates the strong bonding character inside this chain. It is worth mentioning that this tunnel structure is, a priori, capable of adapting structural rearrangement resulting from different sizes and concentrations of alkali atoms.

TABLE 4
Bond Lengths and Interatomic Distances (Å)
$A_{2-x}V^{5+}_{8-x-2y}V^{4+}_{y}Mo^{6+}_{x+y}O_{21}$ in with A = K, Rb, Cs

	K	Rb	Cs
M1–O7	1.633(4)	1.631(4)	1.630(7)
M1–O6	2.166(4)	2.160(4)	2.168(6)
M1–O3h	2.298(4)	2.317(4)	2.309(7)
M1–O8	1.814(1)	1.818(1)	1.820(1)
M1–O1 (×2)	1.899(1)	1.902(1)	1.898(2)
⟨M1–O⟩	1.952(3)	1.955(4)	1.954(4)
Valence	5.29	5.17	5.28
M2–O5	1.614(4)	1.614(4)	1.613(7)
M2–O4	1.908(4)	1.924(4)	1.909(6)
M2–O3h	2.394(4)	2.399(4)	2.386(6)
M2–O6	2.019(4)	2.023(4)	2.026(6)
M2–O2 (×2)	1.874(1)	1.876(1)	1.869(2)
⟨M2–O⟩	1.947(2)	1.951(5)	1.945(5)
Valence	5.39	5.24	5.42
M3–O9	1.612(4)	1.616(4)	1.611(6)
M3–O1h	2.176(3)	2.190(4)	2.179(6)
M3–O2h	2.416(4)	2.408(4)	2.409(6)
M3–O4	1.732(4)	1.730(4)	1.733(6)
M3–O3 (×2)	1.920(1)	1.922(1)	1.916(2)
⟨M3–O⟩	1.963(3)	1.960(6)	1.961(5)
Valence	5.47	5.10	5.49
M1–M2	3.534(1)	3.536(1)	3.539(1)
M2–M3h	3.607(1)	3.399(1)	3.384(1)
M3h–M1	3.263(1)	3.279(1)	3.273(1)
V–O10	1.581(4)	1.591(4)	1.573(6)
V–O6	1.795(4)	1.802(4)	1.784(6)
V–O11k	1.982(3)	1.989(4)	1.978(7)
V–O11 (×2)	1.900(1)	1.897(1)	1.895(2)
⟨V–O⟩	1.832(3)	1.835(5)	1.825(5)
Valence	4.97	4.93	5.07
V–O7	2.688(3)	2.698(4)	2.724(6)
V–Vk	3.051(1)	3.040(1)	3.039(2)
A–O5 (×2)	3.492(6)	3.406(4)	3.442(6)
A–O10 (×2)	2.681(4)	2.736(3)	2.781(4)
A–O9i (×2)	3.044(4)	3.119(4)	3.127(6)
A–O4i (×2)	3.679(4)	3.727(7)	3.745(6)
A–O5i (×2)	2.876(4)	2.908(4)	2.943(4)
A–O7k	3.370(4)	3.491(5)	3.474(7)
A–Ai	3.830(9)	3.596(4)	3.589(4)
A–A	3.6340(2)	3.6340(2)	3.6300(3)

i: $-x, y, 1-z$. h: $\frac{1}{2}-x, \frac{1}{2}+y, \frac{3}{2}-z$. k: $\frac{1}{2}-x, \frac{1}{2}+y, \frac{1}{2}-z$.

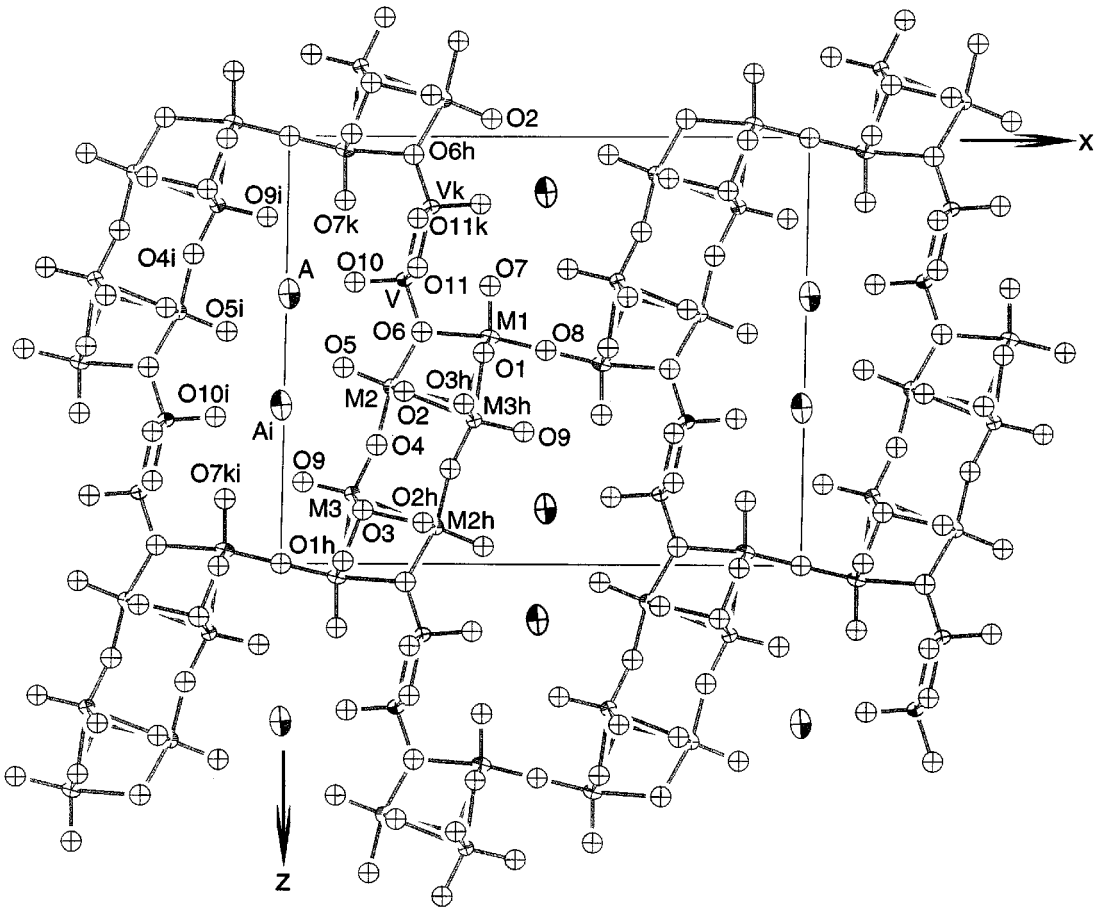

FIG. 1. ORTEP representation of $A_x(Mo,V)_8O_{21}$ structure with atom labels projected onto the (010) plane.

Indeed, nothing prevents the rotation of the double chains VO_5 around their 2_1 axis—the oxygen atoms O6 and O6h playing a knee points role—with the concomitant rigid body shift of the $[M_3O_{19}]_n$ layers along the $[\bar{1}01]$ direction.

The A atoms in the tunnels (with respect to stoichiometries found in this study) are in monocapped pentagonal prisms, A[O5O5iO4iO9iO10]$_2$O7k (A and O7k in $y = 0$ and oxygen pentagons in $y = \pm\frac{1}{2}$ coordinates), see Fig. 3. AO_{11} polyhedra share a rectangular face O5O5iO5iO5 (twofold axis in the middle of O5-O5i) with AiO_{11}. A–Ai distances around 3.6 Å in Rb^+ and Cs^+ and 3.83 Å in K^+ phases appear not to be large enough to accommodate more than one atom per y level and hence an occupancy less than 50%, a situation similar to the one found in the tunnels of the β-$A_xV_2O_5$ vanadium bronzes (Fig. 2b).

Chemical Formula

Based on the fine details given by the structure determination a precise and representative formula of this new family of compounds grossly represented by $A_x(Mo,V)_8O_{21}$ can be extracted. If the alkali sites A were fully occupied the stoichiometric oxidized formula would be $A_2V_8O_{21}$, i.e., an alkali vanadate V. The nonstoichiometry in A cations implies the presence of Mo(VI) to ensure the perfect balance of charges; it gives $A_{2-x}\,Mo_x^{6+}V_{8-x}^{5+}O_{21}$. The site occupancy τ_A for alkali cation sites results in the x value: $x = 2 - 2\tau_A$ (see Table 3). The structural refinements show that in all three phases the amount of molybdenum in the three $M1$, $M2$, and $M3$ sites surpass this x value while the last metallic site is fully devoted to vanadium. If m designates the total amount of molybdenum its value is $m = 2(\tau1 + \tau2 + \tau3)$; there is an excess y of Mo in the crystals: $m = x + y$. We know that Mo^{6+} is perfectly stable versus V^{4+}; the representative phases documenting this assertion are found in the same Mo–V–O phase diagram in the form of $V_{2-x}Mo_xO_5$ phases (with a large homogeneity range $0 < x < 0.60$) (11) and the compound $MoVO_5$ (12) with V^{4+} in square pyramids and Mo^{6+} in tetrahedra. Then, when there is a y excess of Mo^{6+} it is accompanied by the same amount y of V^{4+} and there-fore $2y$ of V^{5+} are substituted; it is the

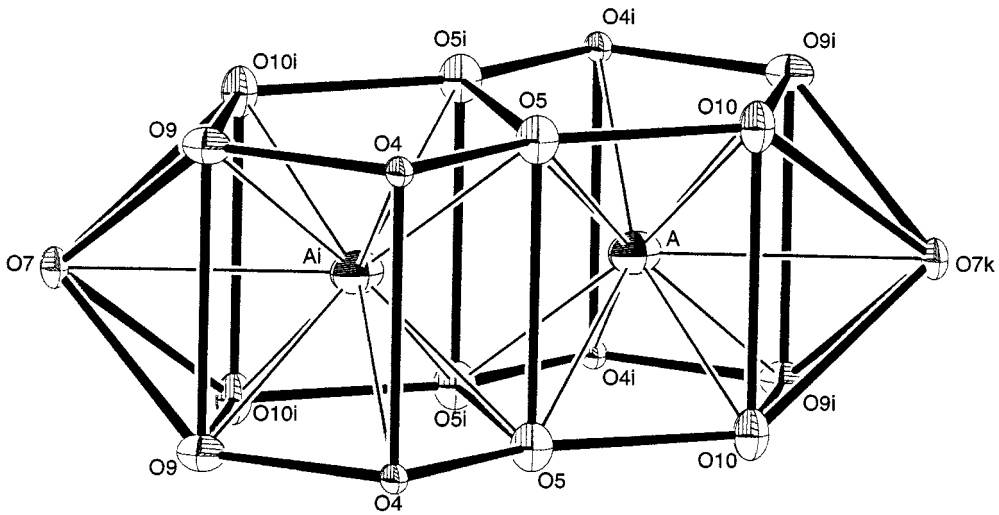

FIG. 2. Coordination polyhedra of alkali atoms (displacement ellipsoids are shown at 85% probability level).

coupled substitution: $y\mathrm{Mo}^{6+} + y\mathrm{V}^{4+} \Rightarrow 2y\mathrm{V}^{5+}$. The general formula of these new phases can then be written:

$$A_{2-x}\mathrm{Mo}^{6+}_{x+y}\mathrm{V}^{5+}_{8-x-2y}\mathrm{V}^{4+}_{y}\mathrm{O}_{21} \text{ with } A = \mathrm{K}^+, \mathrm{Rb}^+, \mathrm{Cs}^+.$$

The x and y values and the corresponding formulas are given in Table 3.

DISCUSSION AND CONCLUSION

The general network of this new family presents some structural similarities with a number of other vanadate bronzes such as β-$\mathrm{Na}_x\mathrm{V}_2\mathrm{O}_5$ (13), $\mathrm{Li}_{1+x}\mathrm{V}_3\mathrm{O}_8$ (14), and γ-$\mathrm{Li}_x\mathrm{V}_2\mathrm{O}_5$ (15). It is interesting to see in Fig. 2 that the VO_5 square pyramid double chains, noted $[\mathrm{V}_2\mathrm{O}_6]_n$, are the basic units that ensure the cohesion of these networks by linking structural entities, very complex in the case of $A_x(\mathrm{Mo,V})_8\mathrm{O}_{21}$ phases and with γ-$\mathrm{LiV}_2\mathrm{O}_5$ that can be regarded as an extreme case since it is formed only by corner-sharing $[\mathrm{V}_2\mathrm{O}_6]_n$ double chains. One of the main structural features of these compounds is that it is possible to obtain frameworks with tunnel structures as well as layered compounds.

In the β phase, capable of accommodating several kinds of atoms in its tunnels (alkali, alkali earths, Cu, Ag, Pb ...), $[\mathrm{V}_2\mathrm{O}_6]_n$ links the $[\mathrm{V}_4\mathrm{O}_{11}]_n$ layers formed by the same quadruple chains sharing corners (Fig. 2b). It is noted that for large inserted cations, i.e., Na^+, K^+, Rb^+, Sr^{2+}, Pb^{2+}, ... the crystallographic site occupancy factor is lower than 50%. In $\mathrm{Li}_{1+x}\mathrm{V}_3\mathrm{O}_8$ (Fig. 2c), the double string $[\mathrm{V}_2\mathrm{O}_6]_n$ connects quadruple chains of $[\mathrm{VO}_6]$ octahedra building up a $[\mathrm{V}_3\mathrm{O}_8]_n$ layer, lithium cations being intercalated in between, assuming the stability of the network. As already mentioned, these $[\mathrm{V}_2\mathrm{O}_6]_n$ strings built up also the layered structure of the γ-$\mathrm{Li}_x\mathrm{V}_2\mathrm{O}_5$ bronze by corner sharing (Fig. 2d) but in this peculiar case two distinct strings are clearly identified: one $[\mathrm{V}^{4+}_2\mathrm{O}_6]_n$ in V1 and one $[\mathrm{V}^{5+}_2\mathrm{O}_6]_n$ in V2. The details of the V–O bonding, reported in Table 5, allow us to appreciate and to compare the characteristics of these strings with our new $A_{2-x}\mathrm{Mo}^{6+}_{x+y}\mathrm{V}^{5+}_{8-x-2y}\mathrm{V}^{4+}_{y}\mathrm{O}_{21}$ phases.

It is worth mentioning that a last structural type could be formed of isolated $[\mathrm{V}_2\mathrm{O}_6]_n$ strings. This has indeed been observed in phases like KVO_3, $\mathrm{H}_2\mathrm{O}$ (16), or $\mathrm{CaV}_2\mathrm{O}_6$ (17). However, in such cases the square pyramid (SP) distorts toward the trigonal bipyramid (TBP), the two V^{5+}–O bonds directed toward the K^+ or Ca^{2+} ions being extremely short.

If potassium and rubidium phases have close formulas, both in alkali insertion and molybdenum substitution, smaller values are observed for corresponding variables in the cesium phase. In order to appreciate the possible distribution of charges in the $M\mathrm{O}_6$ and VO_5 polyhedra, we performed bond-valence-sum analysis (18). To make such calculations an r_0 value for $\mathrm{V}^{4,5+}$ was extrapolated taking into account the ratio $\mathrm{V}^{4+}/\mathrm{V}^{5+}$ for each phase; it gives for vanadium r_0(K or Rb) = 1.801 and r_0(Cs) = 1.802. For each $M\mathrm{O}_6$ octahedron the ratio Mo/V was respected. The calculated valences in the various polyhedra are summarized in Table 5.

It is assumed from this bond valence analysis that V^{5+} are preferentially located in the VO_5 square pyramids of the infinite string $[\mathrm{V}_2\mathrm{O}_6]_n$. Characteristics of this vanadium bonding, i.e., $\langle$V–O$\rangle$ distances and $d_\perp$ (distance of V to the oxygen basal plane of SP), are compared with the ones in $\mathrm{V}_2\mathrm{O}_5$, a pure V^{5+} compound, γ-$\mathrm{LiV}_2\mathrm{O}_5$ bronze in which there are two distinct $[\mathrm{V}^{5+}_2\mathrm{O}_6]_n$ and $[\mathrm{V}^{4+}_2\mathrm{O}_6]_n$ strings, δ-$\mathrm{LiV}_2\mathrm{O}_5$ in which there are $[\mathrm{V}^{4.5+}_2\mathrm{O}_6]_n$ strings, and $\mathrm{MgV}_2\mathrm{O}_5$, where the strings are pure $[\mathrm{V}^{4+}_2\mathrm{O}_6]_n$. Both

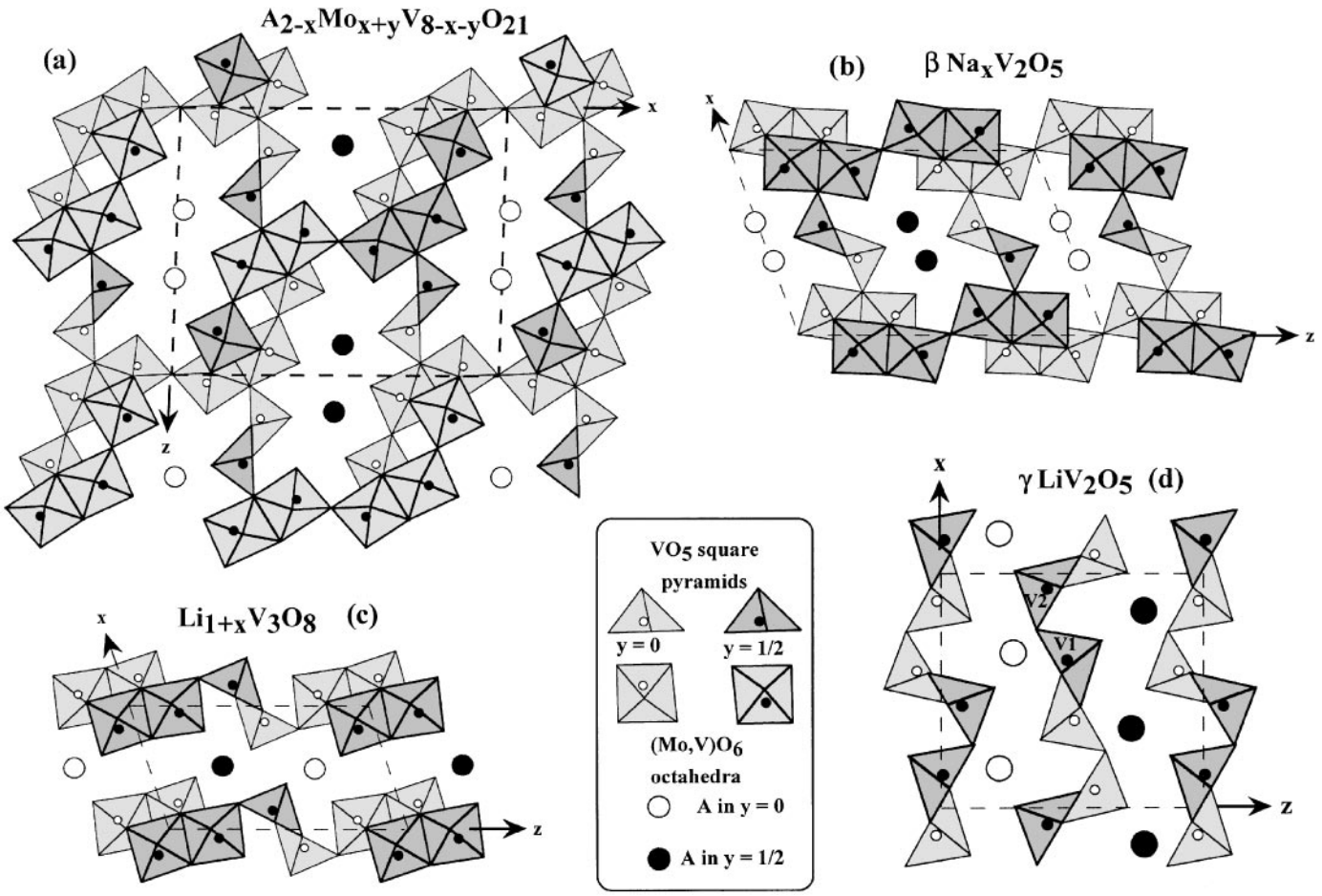

FIG. 3. Idealized projections of (a) $A_{2-x}Mo_{x+y}V_{8-x-y}O_{21}$, (b) β-$Na_xV_2O_5$, (c) $Li_{1+x}V_3O_8$, and (d) γ-LiV_2O_5 structures.

TABLE 5

Average ⟨V–O⟩ Bond Lengths (Å), V–V Interatomic Distances (Å), and $d_\perp$ (Å) Distance of V (with Its Formal Charge) to the Basal Plane in VO_5 SP in Various Vanadium Oxide Compounds

Phases	⟨V–O⟩ (Å)	V–V (Å)	$d_\perp$ (Å) in SP	Ref.
KVO_3, H_2O	1.830	3.140	TBP	(16)
CaV_2O_6	1.826	3.080	TBP	(17)
$Li_{1+x}V_3O_8$	1.840	3.121	(V^{5+}), 0.597	(14)
β-$Na_xV_2O_5$	1.832	3.058	(V^{5+}), 0.462	(13)
V_2O_5	1.823	3.081	(V^{5+}), 0.470	(19)
γ-LiV_2O_5	1.826	3.193	(V^{5+}), 0.539	(15)
	1.876	3.002	(V^{4+}), 0.636	
α'-NaV_2O_5	1.852	3.038	($V^{5,4+}$), 0.562	(20)
δ-LiV_2O_5	1.846	3.035	($V^{5,4+}$), 0.548	(21)
MgV_2O_5	1.894	2.976	(V^{4+}), 0.666	(21)
$K_x(Mo,V)_8O_{21}$	1.832	3.051	(V^{5+}), 0.470	This work
$Rb_x(Mo,V)_8O_{21}$	1.835	3.042	(V^{5+}), 0.471	This work
$Cs_x(Mo,V)_8O_{21}$	1.825	3.039	(V^{5+}), 0.468	This work

bond lengths and valence calculations are in favor of such a hypothesis.

In summary, vanadium–molybdenum mixed bronzes of formula $A_x(Mo,V)_8O_{21}$ ($A = K^+, Rb^+, Cs^+$) have been isolated by a new synthesis approach which involves using the layered compound $(Mo_{0.3}V_{0.7})_2O_5$ as starting material. These compounds present a crystal structure related to other vanadium bronzes with the presence of large tunnels where the alkali atoms are located. Interesting ionic conductivity properties are expected as in the case of β- and β'-$A_xV_2O_5$ phases.

REFERENCES

1. P. Millet, J. Y. Henry, F. Mila, and J. Galy, *J. Solid State Chem.* **147,** 676 (1999).
2. K. Waltersson and B. Forslund, *Acta Crystallogr. B* **33,** 780 (1977).
3. K. D. Hammonds, H. Deng, V. Heine, and M. T. Dove, *Phys. Rev. Lett.* **78,** 3701 (1997).

4. K. D. Hammonds, V. Heine, and M. T. Dove, *J. Phys. Chem. B* **102,** 1759 (1998).
5. R. L. Withers, P. Millet, and Y. Tabira, *Z. Kristallogr.* **215,** 357 (2000).
6. L. Kihlborg, *Acta Chem. Scand.* **21,** 2495 (1967).
7. "Collect" data collection software, Nonius B.V., 1998.
8. A. Altomare, G. Cascarano, C. Giacovazzo, A. Cuagliardi, M. C. Burla, A. Polidori, and M. Camalli, *J. Appl. Crystallogr.* **27,** 435 (1994).
9. G. M. Sheldrix, "SHELXL-96, Program for the Refinement of Crystal Structures." University of Göttingen, Germany, 1996.
10. R. H. Blessing, *J. Appl. Crystallogr.* **30,** 421 (1997).
11. J. Darriet, J. Galy, and P. Hagenmuller, *J. Solid State Chem.* **3,** 596 (1971).
12. H. A. Eick and L. Kihlborg, *Nature* **211,** 515 (1966).
13. A. D. Wadsley, *Acta Crystallogr.* **8,** 695 (1955).
14. A. D. Wadsley, *Acta Crystallogr.* **10,** 261 (1957).
15. J. Galy, J. Darriet, and P. Hagenmuller, *Rev. Chim. Minér.* **8,** 509 (1971).
16. C. L. Christ, J. R. Clark, and H. T. Evans, *Acta Crystallogr.* **7,** 801 (1954).
17. J. C. Bouloux, G. Perez, and J. Galy, *Bull. Soc. Fr. Miner. Cristallogr.* **95,** 130 (1972).
18. I. D. Brown and D. Altermatt, *Acta Crystallogr. B* **41,** 244 (1985).
19. R. Enjalbert and J. Galy, *Acta Crystallogr. C* **42,** 1467 (1986).
20. A. Meetsma, J. L. de Boer, A. Damascelli, J. Jegoudez, A. Revcolevschi, and T. T. M. Palstra, *Acta Crystallogr. C* **54,** 1558 (1998).
21. P. Millet, C. Satto, Ph. Sciau, and J. Galy, *J. Solid State Chem.* **136,** 56 (1998).